Front. Earth Sci. 2021, 15(2): 378–394
https://doi.org/10.1007/s11707-021-0922-9

RESEARCH ARTICLE

Diagenesis of shale and its control on pore structure, a case study from typical marine, transitional and continental shales

Weidong XIE[1], Meng WANG (✉)[2], Hua WANG[1], Ruying MA[3], Hongyue DUAN[2]

1 School of Earth Resources, China University of Geosciences, Wuhan 430074, China
2 Low Carbon Energy Institute, China University of Mining and Technology, Xuzhou 221008, China
3 College of Geology and Mining Engineering, Xinjiang University, Urumqi 830000, China

Abstract Due to discrepancies in pore structure, the productivity of shale gas reservoirs under different diagenesis stages varies greatly. This study discussed the controlling of sedimentation and diagenesis on shale pore structure in typical marine, transitional, and continental shales, respectively. Continental shale samples from the Shuinan Formation, Jiaolai Basin, transitional shale samples from the Taiyuan, Shanxi and Xiashihezi Formations, Ordos Basin, and marine shale samples from the Longmaxi Formation, Sichuan Basin, were collected. Scanning electron microscope with argon ion polishing, high-pressure mercury injection, and low-temperature nitrogen adsorption experiments were conducted to acquire pore structure parameters. And the diagenetic stage of the reservoir was classified according to thermal maturity, organic geochemical parameters, and mineral composition. Our results exhibit that continental, transitional, and marine shales are period A, period B of the middle diagenetic stage, and the late diagenetic stage, respectively. For pore structure, micropore (0–2 nm) and mesopore (2–50 nm) controlled pore volume and specific surface area of transitional and marine shales, and specific surface area of continental shale have similar results, while micropore, mesopore, and macropore (>50 nm) all have a significant proportion of pore volume in continental shale. The pore structure characteristics and controlling factors exhibit a pronounced difference in different diagenesis stages, the compaction and cementation in period A of the middle diagenesis stage is relatively weak, intergranular pore and interlayer pore of clay minerals are well preserved, and moldic pore and dissolved pore developed as well; organic matter is in high maturity in period B of the middle diagenesis stage, organic matter pore developed correspondingly, while the intergranular pore developed poorly affected by compaction, notably, the carbonate is negligible in transitional shale, and the interlayer pore of clay minerals are well preserved with weak cementation; while dissolution and metasomatism controlled the pore structure in the late diagenesis stage in marine shale, the primary pores were poorly preserved, and the organic matter pore and carbonate dissolved pore developed. Results from this work are of a specific reference for shale gas development under different diagenesis stages.

Keywords shale gas reservoirs, diagenesis stage, pore structure, controlling factors

1 Introduction

Due to its enormous recoverable reserves and exploration potential, the development of shale gas reservoirs has captured extensive attention worldwide (Li et al., 2009; Barth, 2013; Liu et al., 2015). As shale is a porous medium with strong heterogeneity, complicated occurrence and migration mechanism of methane, the shale pore structure is a crucial parameter affecting methane productivity (Li et al., 2019, 2020). Pores in shale can be divided into the primary pore and secondary pore according to pore type and formation stage. The pore morphology and structural characteristics are transformed by diagenesis (Katsube and Williamson, 1994; Liang et al., 2017). Namely, the variability of diagenetic evolution leads to the difference in the pore structure. The type and proportion of primary and secondary pores are also significantly different, which affects the occurrence space and storage capacity of methane in shale (Xiong et al., 2016; Long et al., 2017; Xie et al., 2021). In the standard of the petroleum and natural gas industry in China (SY/T 5477-2003), the diagenetic stages can be divided into five stages, which are the syngenetic stage, early diagenetic stage, middle diagenetic stage, late diagenetic stage, and epigenetic

Received January 18, 2021; accepted June 3, 2021

E-mail: wangm@cumt.edu.cn

stage, which is based on the distribution characteristics of authigenic minerals, the completion of smectite- mixed I/S- illite and smectite- mixed C/S- chlorite transformation sequences in clay minerals, the thermal maturity and paleotemperature of organic matter in shale. The diagenesis consists of compaction, cementation, metasomatism, recrystallization, leaching, and dissolution. Compaction, cementation, and recrystallization will cause the shale compaction, which leads to the decreasing of the pore porosity and amounts, pore plugging, and mainly affecting the intergranular pores (Tian et al., 2014; Fan et al., 2019). Leaching and dissolution dissolve the soluble components in shale, destroy their integrity and compactness, and form a certain amount of secondary pore (Zhang et al., 2018; Guo et al., 2019). In addition, the pores formed by hydrocarbon generation of organic matter also contribute to the pore structure of shale during diagenesis evolution.

Additionally, with the deepening of diagenetic evolution, a large number of secondary pores will form in kerogen, which is one of the significant contributors to pores in shale. It includes dissolved pore, microfissure, and hydrocarbon generation pores in organic matter, and the latter is dominant (Curtis et al., 2012; Song et al., 2016). When kerogen reaches a particular evolutionary stage, gaseous hydrocarbons are generated, the structure of organic matter is destroyed, and accompanied by the formation of a large number of pores.

The diagenesis controlling on the shale pore structure leads to the differences in the pore structure of organic matter and mineral compositions in different diagenetic stages. Specifically, Total organic carbon (TOC) and clay content presented a positive correlation with pore volume (PV) and specific surface area (SSA) caused by their molecular structure or micropores. Hydrocarbon generating pores dominate the former with various pore morphology. The latter is mainly interlayer pore and microfissure (Xie et al., 2021). Brittle minerals such as quartz, feldspar, and carbonate are generally unfavorable to the development of pores, exhibiting negative correlation, while their content is the critical factor affecting the fracturing performance (Zhao et al., 2016; Yang et al., 2018). Also, the pore structure is also affected by compaction, cementation, pressure solution, dissolution, and metasomatism in diagenesis evolution (Zhang et al., 2018; Guo et al., 2019). Hence, it is indispensable to explore the pore structure characteristics, influencing factors, and controlling mechanism of the shale reservoirs in different diagenesis stages and characterize the impact of pore structure parameters on shale gas productivity.

In this study, three types of shale samples were collected. The continental shale samples are from the Shuinan Formation (K_1s) (Jiaolai Basin). The transitional shale samples are from the Taiyuan (C_2–P_1t), Shanxi (P_1s) and Xiashihezi Formations (P_1x) (Ordos Basin). The marine shale samples are from the Longmaxi Formation (S_1l) (Sichuan Basin) (Fig. 1). The sedimentary backgrounds of these three sample locations are deep lacustrine facies, transitional facies, and deep shelf facies, respectively. Fluid injection experiments and gas adsorption experiments were employed to characterize PV and SSA. And the diagenetic stages of the three types of shales were clarified, referring to the test results of R_o, the influence of organic geochemical parameters and mineral composition on PV and SSA were discussed. In addition, the controlling mechanism of the diagenetic stage on pore structure was discussed. The results highlight the pore structure characteristics of shale reservoirs in different diagenesis stages and the contribution of micropore, mesopore, and macropore, which provides references for shale gas exploration, development, and theoretical research.

2 Samples and experiments

2.1 Sample collection

In this investigation, shale samples were collected from three petroliferous basins in China. The Jiaolai Basin (continental shale), Ordos Basin (transitional shale), and Sichuan Basin (marine shale) (Fig. 1). The Jiaolai Basin, located in the Shandong Province, eastern China, belongs to the Mesozoic continental residual basin controlled and reformed by the middle and late Mesozoic fault activities. The continental shale gas reservoir of the Shuinan Formation in the Laiyang Group, deposited during the Early Cretaceous, is the product of lacustrine deposition in the peak period of fault basin development. The Shuinan Formation is mainly composed of the delta, semi-deep lake, deep lake sedimentary facies (Qiu, 2018). The lithology of K_1s (200–430 m) comprises grayish-black, gray siltstone, and shale with limestone, having an abundance of plant fossils. The Ordos Basin, located in the mid-west of China, is a cratonic basin formed by the superposition of the Paleozoic platform and the Meso Cenozoic inland depression basin. This basin is the junction of the east–west structural domain (Chen et al., 2005). The coal measure transitional shale of the Taiyuan, Shanxi, and Xiashihezi Formations are in the Carboniferous–Permian, deposited under a fluvial delta and surface sea sedimentary system. This basin is characterized by a high abundance of organic matter, numerous layers, and large cumulative thicknesses. The Chongqing City lies to the east, on the outer edge of the Sichuan Basin, southwest China. The marine shale of the Longmaxi Formation in the lower Silurian has a wide distribution with a high abundance of organic matter, large thicknesses, and enormous resources (Jiang et al., 2013; Xiong et al., 2015).

Eight drilling samples from the K_1s were collected from the north of the Jiaolai Basin, having a lithology dominated

by grayish-black siltstone and mud shale. Seven transitional drilling shale samples were collected from the southeastern edge of the Ordos Basin, including C_2–P_1t, P_1s, and P_1x, which were black shale mostly. Seven marine shale samples were collected from southeastern Chongqing, situated on a fresh outcrop profile. The lithology of these samples is mainly black siliceous shale (Table 1).

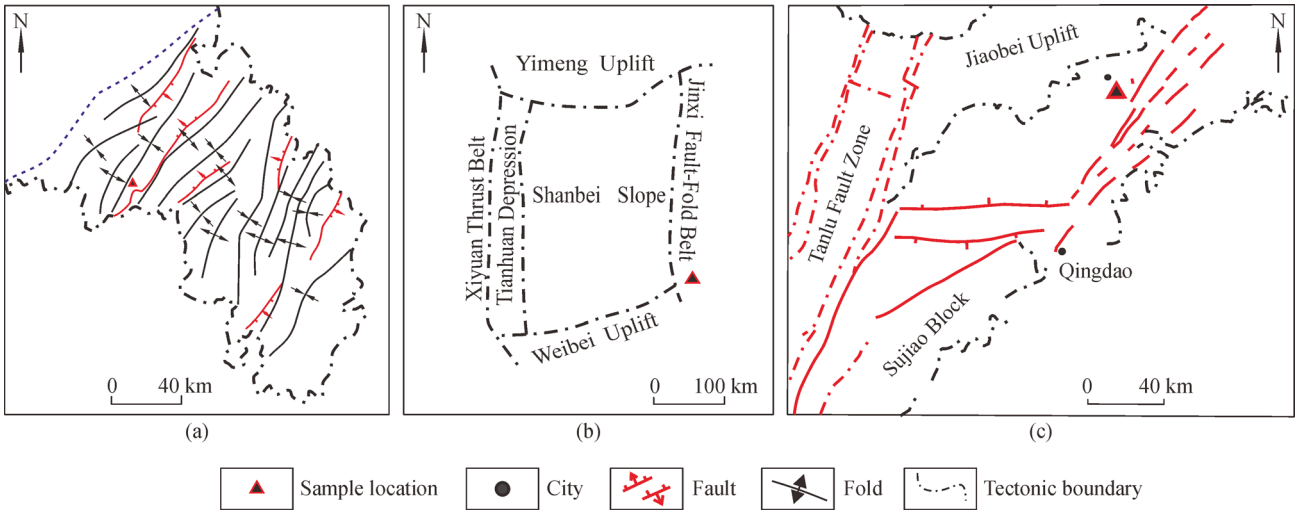

Fig. 1 Sample location of (a) continental shale, (b) transitional shale, and (c) marine shale.

Table 1 Lithology and organic geochemical parameters of continental, transitional, and marine shale samples

Sample ID	Strata	Lithology	TOC/%	R_o/%
JL-1	K_1s	Silty shale	0.13	1.01
JL-2	K_1s	Silty shale	0.5	0.8
JL-3	K_1s	Mud shale	1.42	0.81
JL-4	K_1s	Silty shale	0.28	
JL-5	K_1s	Silty shale	0.5	0.77
JL-6	K_1s	Mud shale	1.58	0.8
JL-7	K_1s	Mud shale	1.42	0.88
JL-8	K_1s	Silty shale	0.53	0.89
SX-1	P_1x	Mud shale	2.31	1.85
SX-2	P_1x	Mud shale	2.58	1.88
SX-3	P_1x	Mud shale	2.65	1.86
SX-4	P_1s	Mud shale	3.36	1.94
SX-5	C_2-P_1t	Mud shale	2.48	1.83
SX-6	C_2-P_1t	Mud shale	1.52	1.9
SX-7	C_2-P_1t	Mud shale	3.08	2.1
CQ-1	S_1l	Carbonaceous shale	5.30	2.6
CQ-2	S_1l	Carbonaceous shale	4.81	2.84
CQ-3	S_1l	Carbonaceous shale	4.96	2.01
CQ-4	S_1l	Carbonaceous shale	4.89	2.31
CQ-5	S_1l	Siliceous shale	2.98	2.5
CQ-6	S_1l	Siliceous shale	2.09	2.32
CQ-7	S_1l	Siliceous shale	1.83	2.66

Notes: P_1x is the Xiashihezi Formation of the Lower Permian, P_1s is the Shanxi Formation of the Lower Permian, C_2–P_1t is the Taiyuan Formation of the Upper Carboniferous- Lower Permian.

2.2 Experiments and methods

According to the International Union of Pure and Applied Chemistry, micropore, mesopore, and macropore classification is defined as having sizes of < 2 nm, 2–50 nm, and >50 nm, respectively (Everett and Koopal, 2001). Pore volume (PV) and Specific surface area (SSA) of the samples were obtained by conducting indirect experimental tests, including high-pressure mercury injection experiments and low-temperature N_2 adsorption experiments. According to the applicability of experiments, micropore and mesopore were characterized by low-temperature nitrogen (N_2) adsorption experiments. Whereas high-pressure mercury injection results characterized macropore. PV was calculated in the Barret-Joyner-Halenda model and SSA in the Brunauer-Emmett-Teller model.

A Quantachrome Autopore 9500 full automatic mercury porosimeter (Manufactured by micromeritics company, America) was applied to measure macropore. The test pressure of this instrument is in the range of 0–60000 psi (413 MPa), and the corresponding pore diameter is in the range of 3 nm–1000 μm. Before analysis, samples were powered into small pieces of about 1 cm^3 and dried at 70°C–80°C for 12 h. During the examination, pressure in the instrument was increased from 0.01 MPa to 413 MPa during the mercury injection stage and decreased during the mercury withdrawal stage. Equipment equilibrium time lasted for 5 s. Additionally, a Tristar II 3020 specific surface physical adsorption instrument (Manufactured by micromeritics company, America) was utilized for the low-pressure N_2 adsorption experiment, having a pore diameter range of 0.35–400 nm. Before analysis, samples were sieved in 40–60 meshes and dried under a vacuum at 150°C for 3 h. Finally, high purity N_2 (purity>99.99%) was used as the adsorbate for analysis.

3 Results and discussion

3.1 Organic geochemical parameters and mineral composition

3.1.1 Organic geochemical parameters

Organic geochemical parameters are the basis of hydrocarbon generating potential of source rocks (Boyer et al., 2006; Burnaman et al., 2009). In this investigation, TOC ranges from 0.13% to 1.58% (0.795% average), 1.52% to 3.36% (2.569% average), and 1.83% to 5.29% (3.835% average) for continental, transitional, and marine shale samples, respectively (Table 1, Fig. 2(a)). Vitrinite reflectance (R_o for short) test results for continental shale samples range from 0.77% to 1.01% (0.85% average), being in a low maturity- maturity stage; 1.83% to 2.1% (1.91% average) in transitional shale samples, being in the high maturity stage; and 2.00% to 2.84% (2.46% average) in marine shale samples, being in the high-over maturity stage (Table 1, Fig. 2(b)). TOC in continental shale samples is lower than those of transitional and marine shale samples, with R_o test results having a similar trend. These results indicate that transitional and marine shale has a higher hydrocarbon generation potential, while continental shale mainly forms oil and wet gas in the "oil window."

According to the Petroleum and Natural Gas Industry Standard of the People's Republic of China (SY/T 5477-2003), R_o of organic matter and smectite-illite and smectite-chlorite transformation sequences clay minerals are widely accepted for the classification of diagenetic evolution stages. With the rise in burial depth, the in situ temperature and pressure increase in the diagenetic stage, and organic matter evolution and clay mineral transformation occur. However, the transformation of clay is not only controlled by the burial depth, temperature, and pressure,

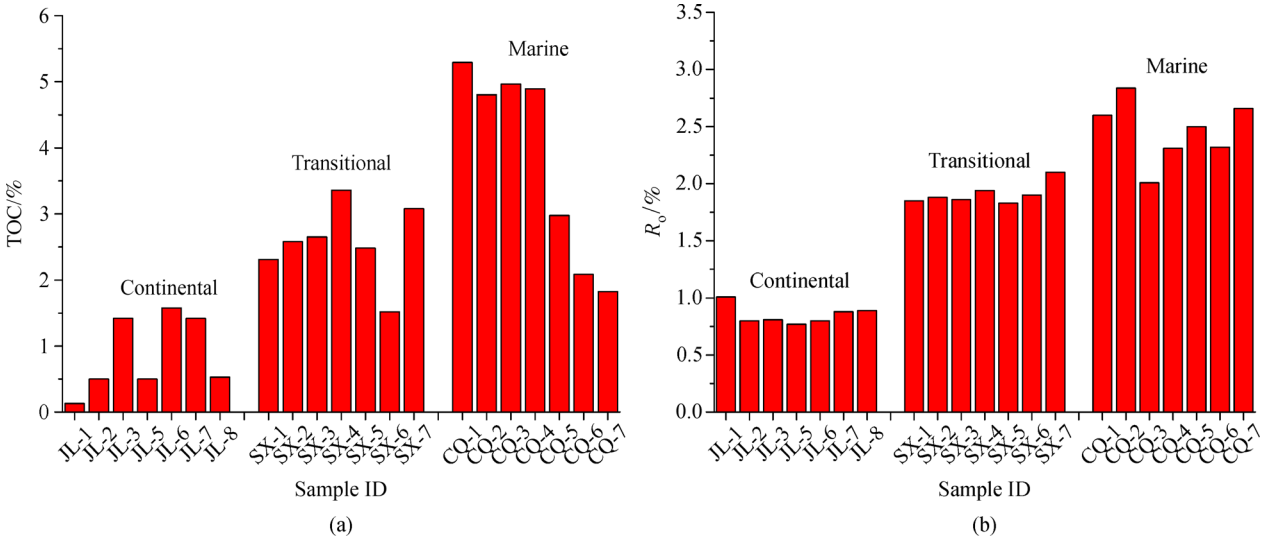

Fig. 2 TOC and R_o test results of continental, transitional, and marine shale samples. (a) The TOC value of shale samples, and (b) the R_o value of shale samples.

but also affected by the concentration of K^+, Mg^{2+}, and Fe^{2+}, etc. Besides, the evolution of organic matter has an apparent inhibitory effect on the transformation of clay in source rocks. Hence the thermal maturity classification scheme is applicable in organic-rich shale. R_o is in the range of 0.77%–1.01% in continental shale, corresponding to period A of the middle diagenetic stage, while the diagenesis is dominated by compaction and cementation. R_o is in the range of 1.83%–2.1% in transitional shale, corresponding to period B of the middle diagenetic stage, as the diagenesis is dominated by dissolution. And R_o is in the range of 2.00%–2.84% in marine shale, corresponding to the late diagenetic stage, while the diagenesis is dominated by dissolution and metasomatism.

3.1.2 Mineral composition

Analysis of mineral composition is presented in Figs. 3 and 4, the compositional maturity of continental shale is the lowest, and the mineral content of eight samples varies greatly, while the mineral content of transitional and marine shale is stable and the floating range is narrow. The specified is as follows: clay, quartz, potash feldspar, plagioclase, and dolomite are the common minerals in continental shale, with an average content of 26.48%, 22.46%, 6.15%, 11.45%, and 23.64%, respectively. Clay and quartz are the dominant minerals in transitional shale with an average content of 57.39% and 35.11%, respectively, and a small proportion of potash feldspar, plagioclase, and dolomite contained with an average content below 5%. Clay, quartz, potash feldspar, feldspar, calcite, dolomite, and pyrite are the common minerals in marine shale samples with an average content of 17.14%, 52.29%, 7%, 11.43%, 4.57%, 4.14%, and 2.71%, respectively. Overall, the composition of continental shale samples is complex and varied. Carbonate, brittle silicate mineral, and clay mineral are the dominant minerals in different samples. Clay mineral is representative in transitional shale samples, followed by brittle silicate mineral. The carbonate content is negligible, while the content of brittle silicate mineral is dominant over 70% in marine shale samples, followed by clay mineral (Fig. 3).

The continental, transitional, and marine shale reservoirs are in period A of the middle diagenetic stage, period B of the middle diagenetic stage, and late diagenetic stage, respectively, which lead to the discrepancy in the transformation process of smectite-mixed I/S- illite. Continental and marine shale samples are dominated by mixed I/S (average values of 11.76% and 10.09%, respectively) and illite (average values of 8.64% and 6.27%, respectively). In contrast, transitional shale contains kaolinite (21% average)>chlorite (14.54% average) >illite (13.67% average)>mixed I/S (8.19% average) (Fig. 4). The three types of shale have completed the first stage of transformation, no smectite has been found, and the S% of mixed I/S was regarded as the evaluation index of transformation degree in the second stage. The diagenetic evolution degree of continental shale is the lowest, and the corresponding S% is the highest; while S% was not detected in transitional shale, similarly, the S% would disappear in the late diagenetic stage in general. However, in this work, the transformation of clay minerals

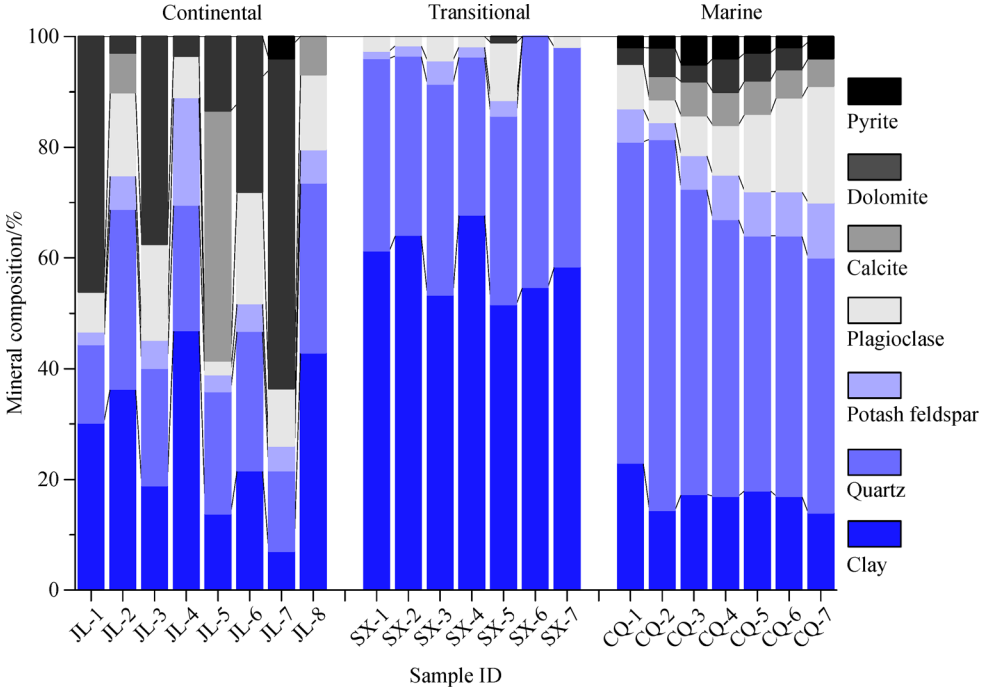

Fig. 3 Mineral composition of continental, transitional, and marine shale samples.

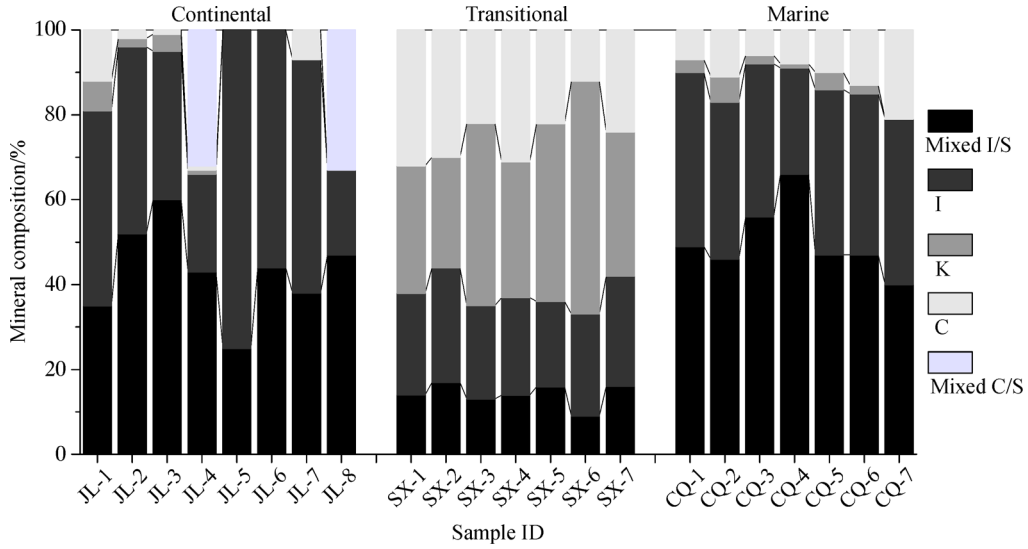

Fig. 4 Mineral composition of clay in continental, transitional, and marine shale samples. Mixed I/S is the mixed layer of illite and smectite, %; I is illite, %; K is kaolinite, %; C is chlorite, %; Mixed C/S is the mixed layer of chlorite and smectite, %.

in marine shale is lower than that of transition shale, which is opposite to the regularity of R_o test results. It is speculated that the organic matter evolution with high-over maturity inhibited the transformation of clay minerals. Zhao and Zhu (2001) and Zhu (2008) reported that the pore water should be an alkaline medium in the transformation sequence of smectite-mixed I/S-illite. However, the organic acids produced in organic matter evolution and decomposition will form a weakly acidic environment in the porous media, which is not conducive to transforming clay minerals. Besides, the acid medium may even promote the reverse transformation of clay minerals.

3.2 Pore structure characteristics of continental, transitional, and marine shales

More than 150 SEM pictures have been shot. Figure 5 exhibits the typical pores in three types of shale samples. According to shale pore classification of Loucks et al. (2009), intergranular pore and interlayer pore of clay minerals, intergranular pore, and microfissure of brittle minerals are primarily in continental shale (Figs. 5(a), 5(b), and 5(c)), mainly in micron-scale; while no large-scale pores development in organic matter (Fig. 5(a)). The hydrocarbon generating pore of organic matter, interlayer pore, and microfissure of clay minerals are the primary in transitional shale, mostly in micron-scale (Figs. 5(d) and 5(e)). Moreover, a few brittle mineral pores were exhibited, consisting of moldic pore and dissolved pore in nano-micron scale (Fig. 5(f)).

In contrast, the organic matter pore was dominated in marine shale and densely distributed in nanoscale with the oval to circular pore morphology (Fig. 5(g)). Influencing by diagenetic compaction and cementation, the pore structure of clay minerals was seriously damaged, causing the unpromising preservation of primary pore (Fig. 5(h)). Furthermore, a certain amount of dissolved pore developed in carbonate on a nano-micron scale (Fig. 5(i)). In a word, the primary pore structure was gradually destroyed with the rise in diagenetic evolution, while the secondary pore, for instance, organic matter pore, dissolved pore, and microfissure, developed increasingly, and the dominant pore types are distinct in each diagenesis stage.

The surface porosity of the three types of shale samples shows the regularity similarly (Fig. 6): the primary pores are dominated in continental shale, most of which are micron-scale. The primary pores and secondary pores are developed simultaneously in the transitional shale, and the pore size is significantly smaller than that of continental shale. The nanoscale secondary pores are primary in the marine shale.

In this investigation, pore structure characteristics were characterized by examining PV (V_1–V_3) and SSA (A_1–A_3); and the former provides accumulation space, the latter provides adsorption sites. In terms of test range advantages, N_2 adsorption test results were selected for micropore and mesopore structure parameters. Mercury injection test results were selected for macropore (Figs. 7 and 8). In continental shale, the average of V_1, V_2, V_3, and V is 0.0013417 cm^3/g, 0.0037919 cm^3/g, 0.00275 cm^3/g, and 0.0078835 cm^3/g, respectively; And the average of A_1, A_2, A_3, and A is 2.2618 m^2/g, 0.5316 m^2/g, 0.0950 m^2/g, and 2.8884 m^2/g, respectively. In transitional shale, the average of V_1, V_2, V_3, and V is 0.0025571 cm^3/g, 0.0094143 cm^3/g, 0.0012271 cm^3/g, and 0.01320 cm^3/g, respectively; And the average of A_1, A_2, A_3, and A is 3.4914 m^2/g, 3.5671 m^2/g, 0.2571 m^2/g and 7.3157 m^2/g, respectively. In marine shale, the average of V_1, V_2, V_3,

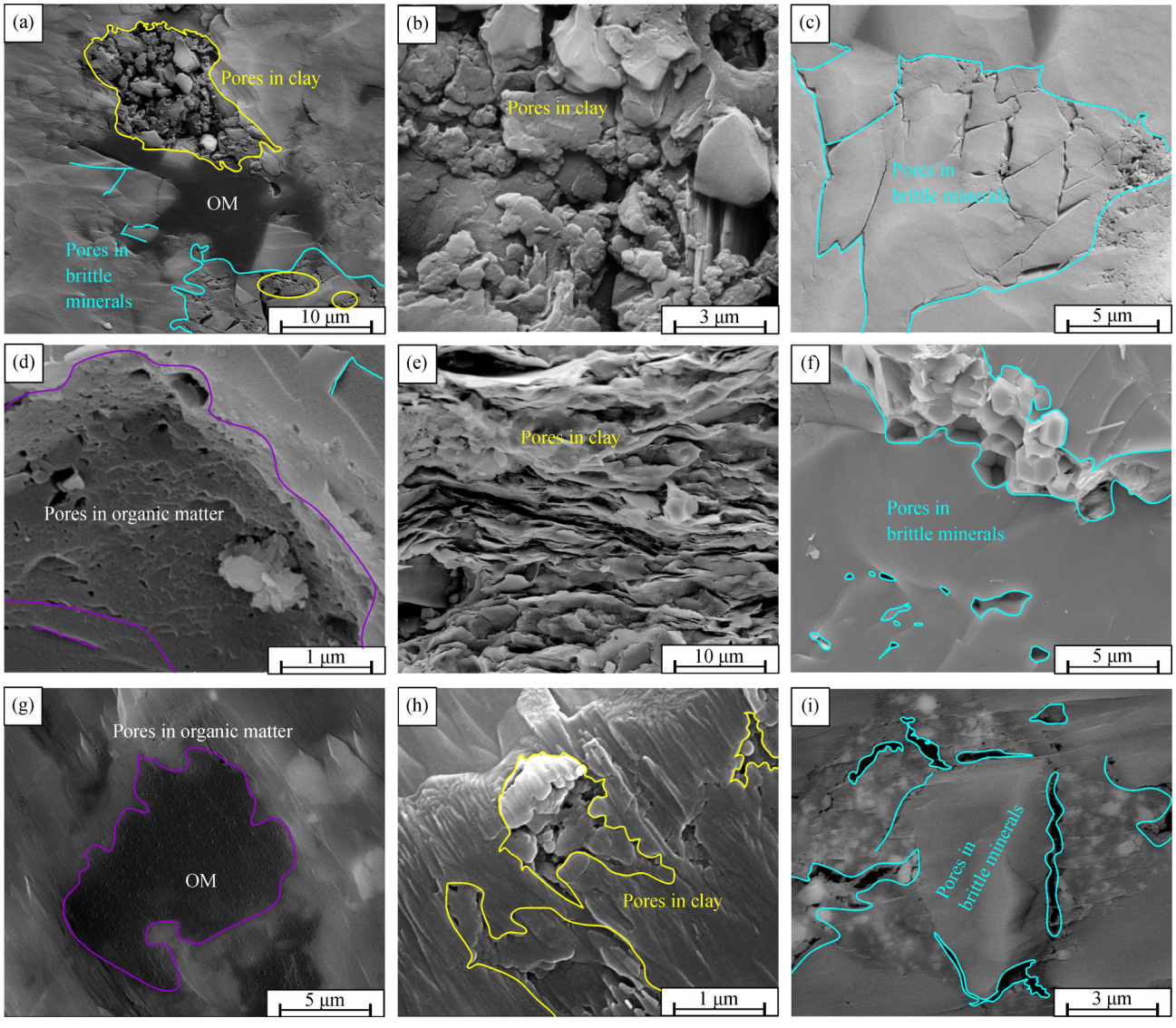

Fig. 5 Scanning electron microscope (SEM) pictures of continental, transitional, and marine shale samples. Continental shale: (a) intergranular pore of clay and brittle minerals; (b) intergranular pore and interlayer pore of clay; (c) intergranular pore and marginal microfissure of brittle minerals. Transitional shale: (d) organic matter pore and microfissure; (e) interlayer pore and microfissure of clay; (f) intergranular pore and moldic pore of brittle minerals. Marine shale: (g) organic matter pore; (h) intergranular pore of clay; (i) dissolved pore and marginal microfissure of brittle minerals.

and V is 0.0029174 cm^3/g, 0.0036503 cm^3/g, 0.0014857 cm^3/g, and 0.0080534 cm^3/g, respectively; And the average of A_1, A_2, A_3, and A is 2.9223 m^2/g, 1.1291 m^2/g, 0.0154 m^2/g, and 4.0668 m^2/g, respectively. In summary, the pore structure of transitional shale is the optimum, with PV and SSA are higher than those of marine and continental shale samples (Figs. 7 and 8). The SSA of the three types of shale samples are all controlled by micropore and mesopore (the proportion of them higher than 95%), the performance of macropore is negligible (the proportion less than 5%). However, the contribution to PV in three types of shale is diverse, mesopore>micropore>macropore in transitional (61%, 20% and 11%, respectively) and marine (43%, 34% and 23%, respectively) shale samples, while mesopore (61%)>macropore (23%)>micropore (16%) in continental shale samples (Figs. 7 and 8).

3.3 Influencing factors of pore structure parameters

The thermal evolution of organic matter in three types of shale is from low to high, and the corresponding diagenetic evolution is likewise, giving distinct increasing to the contribution of organic matter, quartz, feldspar, calcite, and dolomite to pore structure (Gao et al., 2018; Zhang et al., 2018; Chen et al., 2020). In this work, pore structure

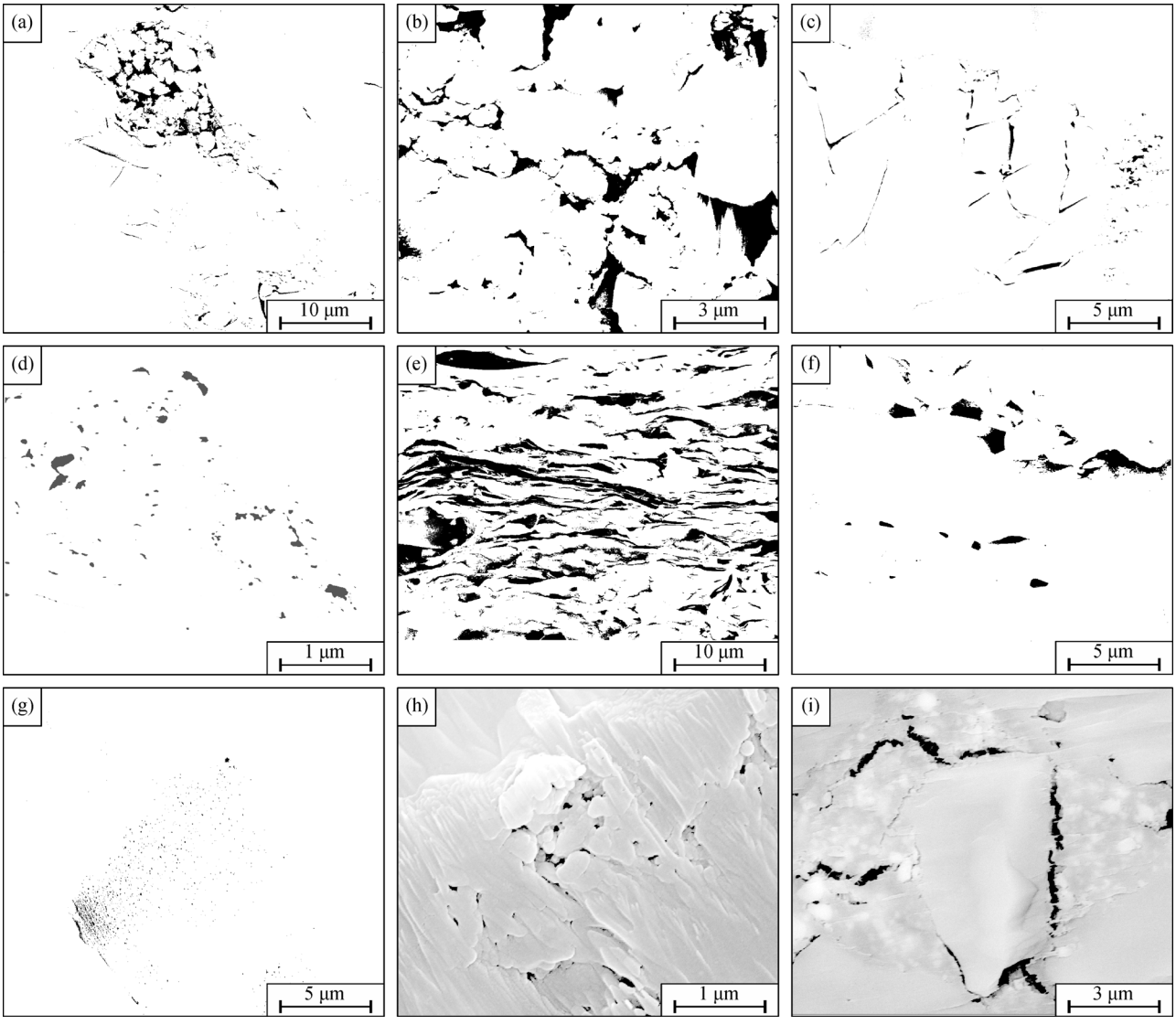

Fig. 6 The pore extraction of SEM pictures (which depicted in Fig. 5) in continental, transitional, and marine shale samples. Continental shale: (a) intergranular pore of clay and brittle minerals; (b) intergranular pore and interlayer pore of clay; (c) intergranular pore and marginal microfissure of brittle minerals. Transitional shale: (d) organic matter pore and microfissure; (e) interlayer pore and microfissure of clay; (f) intergranular pore and moldic pore of brittle minerals. Marine shale: (g) organic matter pore; (h) intergranular pore of clay; (i) dissolved pore and marginal microfissure of brittle minerals.

parameters were represented by PV and SSA, and the contribution of the above factors to PV and SSA was revealed, respectively, in the K_1s, C_2–P_1t–P_1x, and S_1l shale samples (Figs. 9, 10, 11 and 12).

3.3.1 The influence of TOC

A positive linear correlation of PV and SSA versus TOC in marine (R^2 = 0.46896 and 0.5151, respectively) and transitional shale samples (R^2 = 0.4065 and 0.51825, respectively) were recorded; results for the continental shale samples recorded a negative linear correlation among SSA and TOC (R^2 = 0.3071), with no obvious correlation among PV and TOC (R^2 = 0.02488) (Figs. 9(a)–9(f)). R_o of the continental shale samples is below 1.3%, organic matter evolution mainly formed oil and wet gas, which has no obvious contribution to the formation of organic matter pore (Fig. 5(a) and Fig. 6(a)). Analysis of low-maturity lacustrine shale by Wang et al. (2019) also suggested that pores in the organic matter were mostly sporadic dissolved, formed by the dissolution of organic acids, not the hydrocarbon generation pore. By contrast, R_o from our work in transitional shale samples (1.8%–2.1%) was in the stage of high maturity, and R_o values of marine shale samples (2.0%–2.83%) were in the stage of high-over maturity, already passed the limit of oil generation. And a large volume of gaseous hydrocarbon, companied by an ocean of organic matter pore (Figs. 5(d), 5(g), 6(d), and

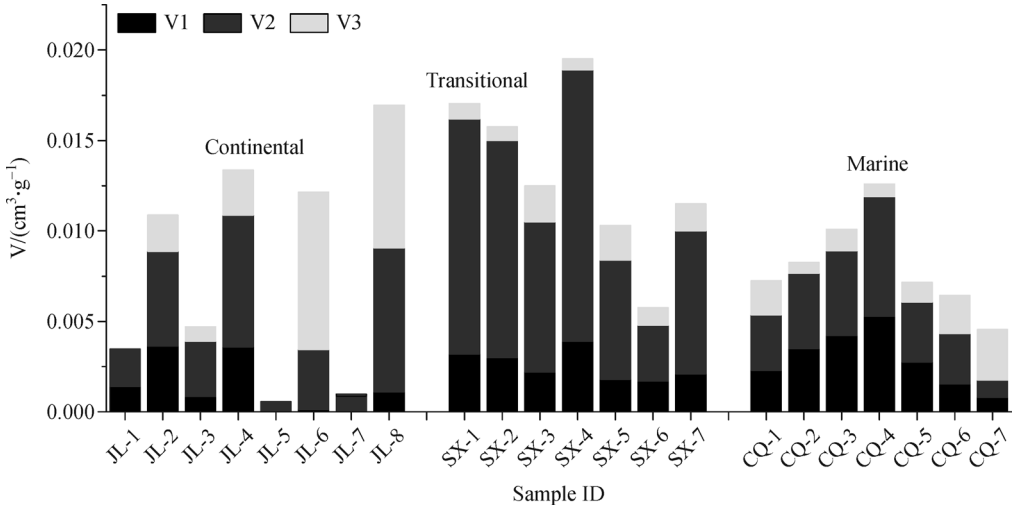

Fig. 7 The contribution of micropore, mesopore, and macropore to PV in continental, transitional, and marine shale samples. V_1 is pore volume of micropore, cm^3/g; V_2 is pore volume of mesopore, cm^3/g; V_3 is pore volume of macropore, cm^3/g; V is the sum of V_1, V_2, and V_3, cm^3/g.

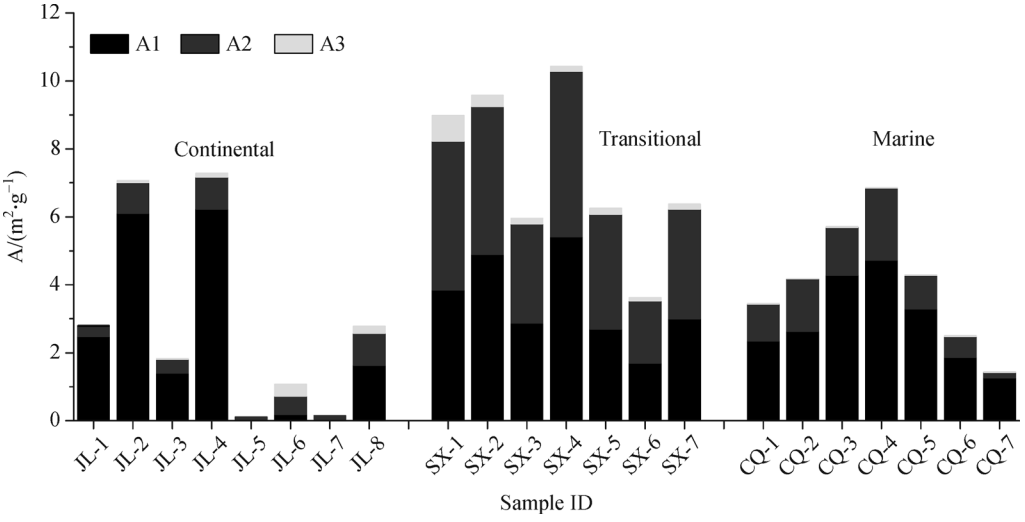

Fig. 8 The contribution of micropore, mesopore, and macropore to SSA in continental, transitional, and marine shale samples. A_1 is the specific surface area of micropore, m^2/g. A_2 is the specific surface area of mesopore, m^2/g. A_3 is the specific surface area of macropore, m^2/g; A is the sum of A_1, A_2, and A_3, m^2/g.

6(g)), was formed under the action of hydrocarbon generating expansion forces. The organic matter abundance is regarded as the pivotal factor of pore structure parameters in highly mature to over mature organic-rich shale (He et al., 2017; Zhao et al., 2017; Yang et al., 2018).

3.3.2 The influence of mineral composition

Clay minerals were regarded as essential shale gas enrichment sites besides organic matter due to the development of interlayer pore (Ji et al., 2012; Chen et al., 2017; Ge et al., 2020). A positive linear correlation was recorded of PV and SSA versus clay content in continental shale samples (R^2 = 0.67977 and 0.82823, respectively) and transitional shale samples (R^2 = 0.64353 and 0.88905, respectively) (Figs. 10(a), 10(b), 10(d), and 10(e)); Correlations for marine shale samples were not pronounced (R^2 = 0.008 and 0.01478, respectively) (Figs. 10(c) and 10(f)). Although clay is a type of inorganic porous medium, our results indicate that the performance of pore structure parameter was various of the K_1s, C_2–P_1t– P_1x, and S_1l shale samples. The reason behind this phenomenon is that diagenetic temperature and pressure of shale increased with the rise in burial depth, and the clay minerals transformed in this process, which included two sequence of smectite- mixed I/S- illite and

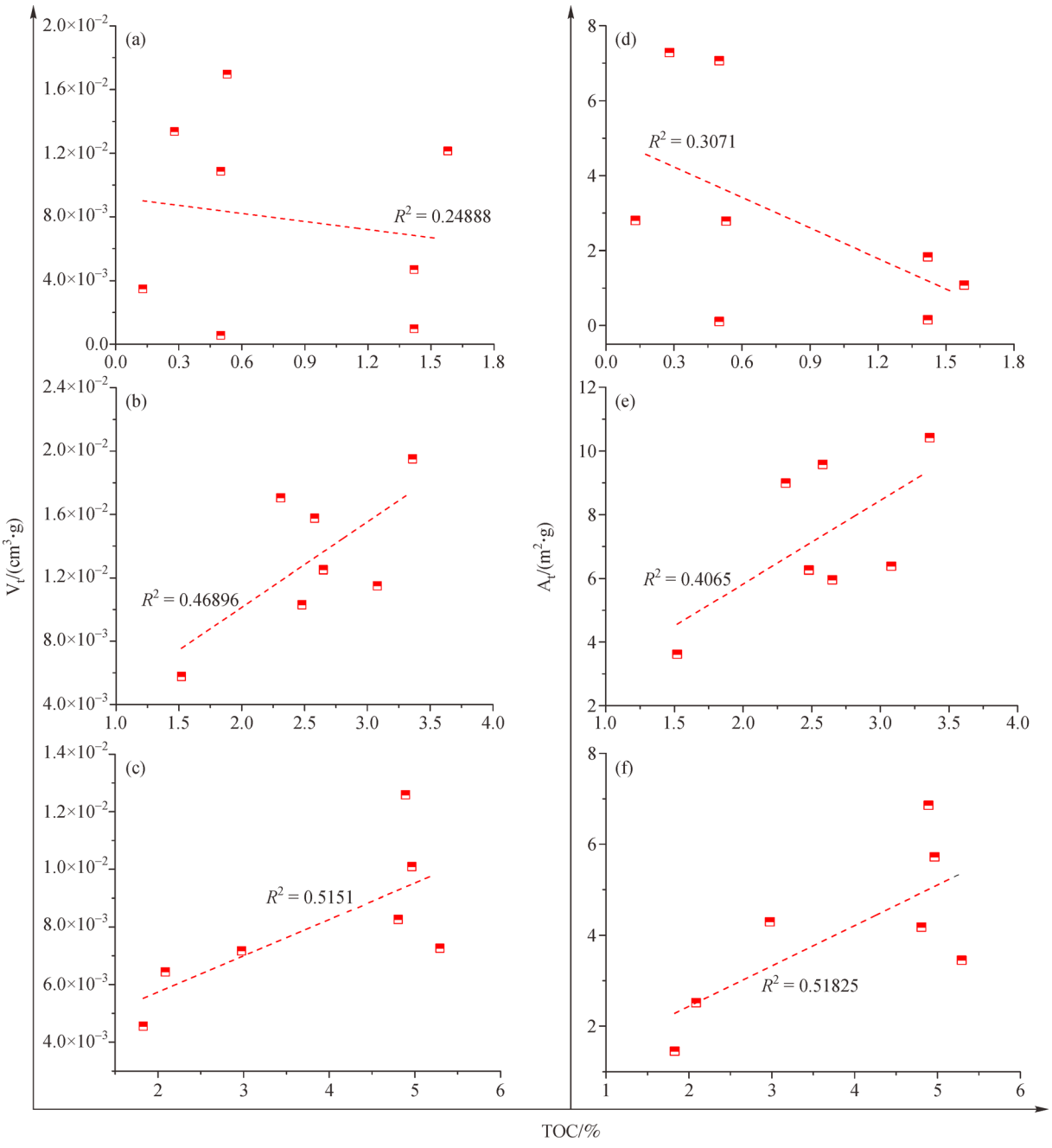

Fig. 9 The correlation of TOC versus PV and TOC versus SSA in continental, transitional, and marine shale samples. (a), (b), and (c) is the correlation of V_t versus TOC in continental, transitional, and marine shale samples, and (d), (e), and (f) is the correlation of A_t versus TOC in continental, transitional, and marine shale samples.

smectite- mixed C/S- chlorite (Colten-Bradley, 1987; Elliott et al., 1999). Also, the transformation of clay minerals is accompanied by the discharge of interlayer water and cations. The lattice spacing becomes smaller, leading to the deterioration of the pore structure and the decrease of surface porosity (Figs. 5(b), 5(e), 5(h), 6(b), 6 (e), and 6(h)). As mentioned above, the evolution of organic matter has a certain inhibitory on the transformation of clay minerals, while it not inhibits the deterioration of pore structure, which is still reflected in the deterioration of pore structure with the rise in diagenetic evolution degree.

Additionally, the higher the degree of evolution, the stronger the compaction and cementation of the reservoir are. The development of the intergranular pore of clay minerals is poor correspondingly, which is not favorable to the reservoir performance of shale. The SEM pictures exhibit the same regularity (Figs. 5(b), 5(e), 5(h), 6(b),

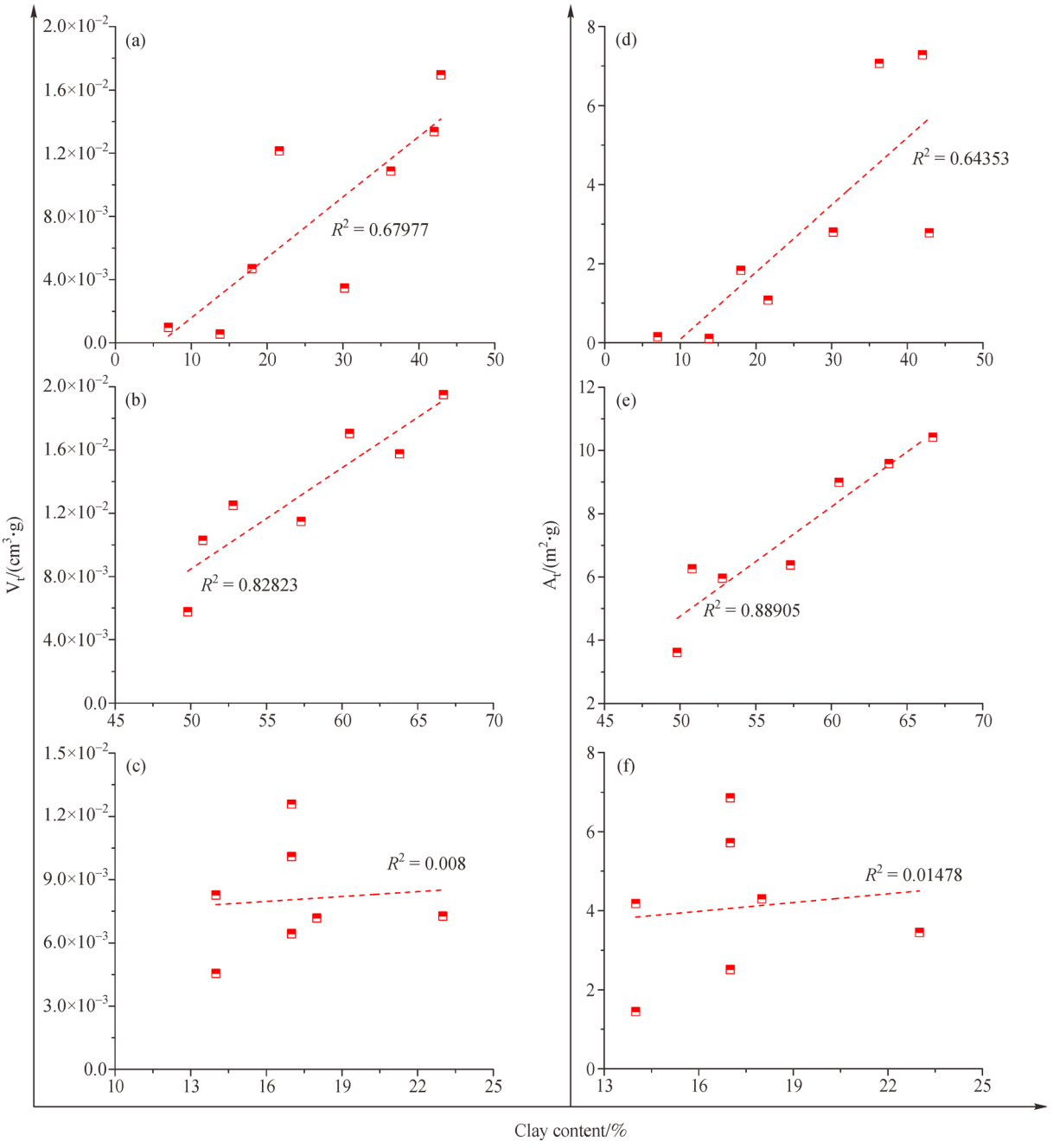

Fig. 10 The correlation of clay content versus PV and SSA in continental, transitional, and marine shale samples. (a), (b), and (c) is the correlation of V_t versus clay content in continental, transitional, and marine shale samples, and (d), (e), and (f) is the correlation of A_t versus clay content in continental, transitional, and marine shale samples.

6(e), and 6(h)).

Quartz and feldspar are the major brittle mineral components of shale, which certainly control the development of shale pore structure. Quartz and feldspar content has a positive linear correlation versus PV and SSA in continental shale (R^2 = 0.72891 and 0.26722, respectively) (Figs. 11(a) and 11(d)); And a linear negative impact on PV and SSA in transitional shale (Figs. 11(b) and 11(c)) (R^2 = 0.48339 and 0.57079, respectively) and marine shale (R^2 = 0.67321 and 0.81698, respectively) (Figs. 11(b) and 11(c)). The pore in feldspar and quartz is mainly intergranular pores and microfissure and a few dissolved pores. Overall, the diagenetic evolution of continental shale is the lowest. Compaction, cementation, and secondary enlargement of quartz and feldspar are the weakest. The primary intergranular pores are optimum preserved correspondingly (Figs. 5(c) and 6(c)).

On the other hand, the intergranular pore of quartz and

feldspar are mostly in micron scale, and the contribution to PV is better than SSA, which leads to the higher correlation fitting degree of the former (Fig. 11(a)). However, due to the stronger compaction, cementation, and secondary enlargement, the intergranular pore is not well preserved in transitional shale and marine shale, while dissolved pore of carbonate and a small amount of pyrite moldic pore, dissolved pore, and microfissure of brittle minerals are found (Figs. 5(f), 5(i), 6(f), and 6(i)). It is generally suggested that brittle silicate minerals are not conducive to the formation of pore structure except for organic quartz in the shale reservoir of the high diagenetic stage (Zhao et al.,

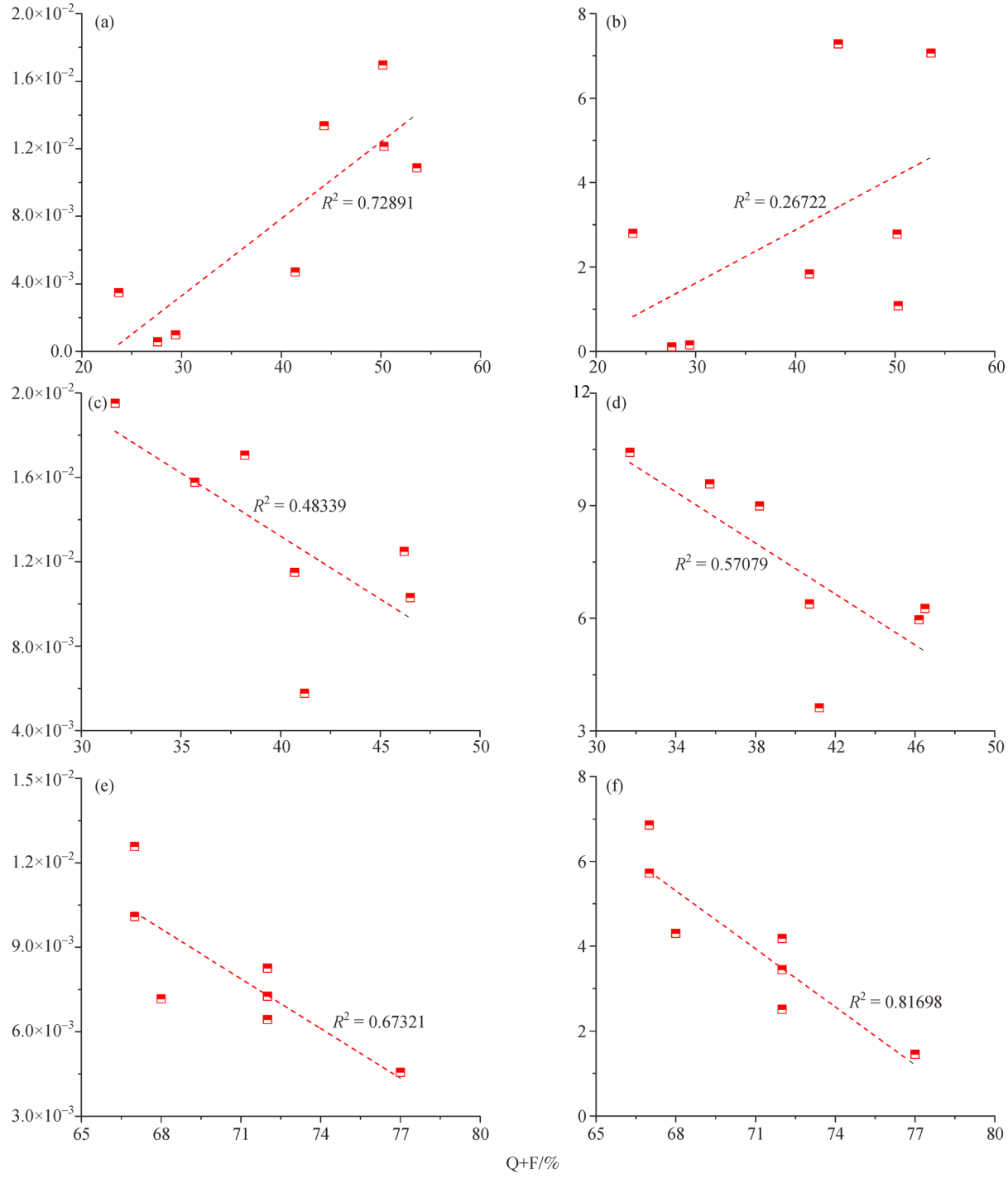

Fig. 11 The correlation of quartz and feldspar content versus PV and SSA in continental, transitional, and marine shale samples. Q is quartz content, %; F is the sum of plagioclase and potash feldspar content, %; (a), (b), and (c) is the correlation of V_t versus the content of Q + F in continental, transitional, and marine shale samples, and (d), (e), and (f) is the correlation of A_t versus the content of Q + F in continental, transitional, and marine shale samples.

2016; Pan et al., 2017; Liu et al., 2019).

Carbonate (calcite and dolomite) is a type of soluble mineral, especially in diagenetic evolution under the action of acid fluid, which can form independent or interconnected dissolution pores. Carbonate is a common mineral composition in continental and marine shale samples, while it is rarely in transitional shale. Only sample SX-5 contains minor dolomite. A negative linear correlation of PV and SSA versus calcite and dolomite content in continental shale samples (R^2 = 0.87605 and 0.64419, respectively) was recorded (Figs. 12(a) and 12(d)). Results for the marine shale samples recorded a weak positive

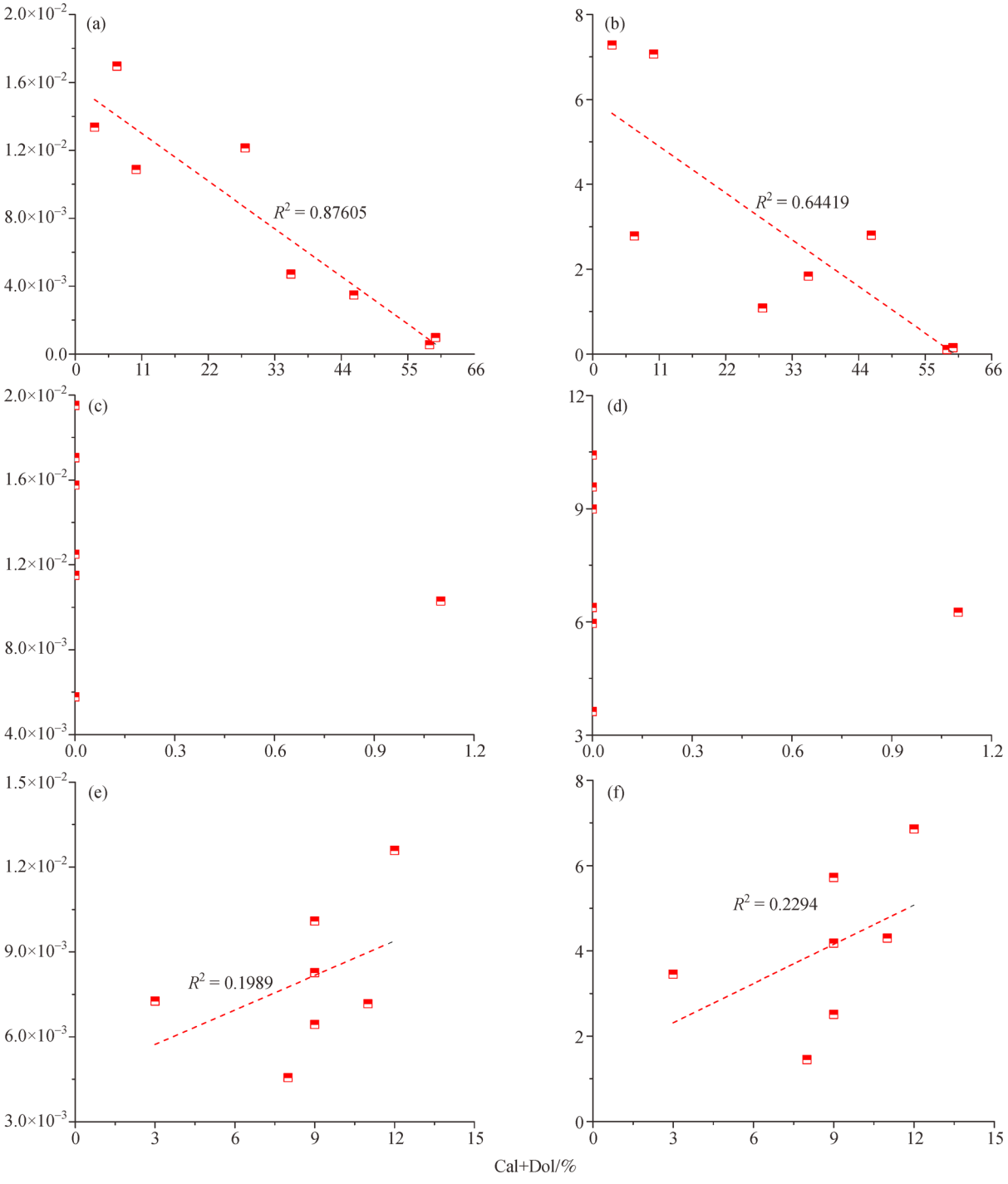

Fig. 12 The correlation of calcite and dolomite content versus PV and SSA in continental, transitional, and marine shale samples. (a), (b), and (c) is the correlation of V_t versus the content of Cal + Dol in continental, transitional, and marine shale samples, and (d), (e), and (f) is the correlation of A_t versus the content of Cal + Dol in continental, transitional, and marine shale samples.

linear correlation of PV and SSA versus calcite and dolomite content (R^2 = 0.1989 and 0.2294, respectively) (Figs. 12(c) and 12(f)). Several reasons are causing the low diagenetic evolution of the continental shale in period A of the middle diagenetic stage. Carbonate is less affected by dissolution, and the dissolved pore is not developed.

Moreover, since the diagenesis of this stage is compacted and cemented primarily, carbonate cement destroyed the original pore structure, resulting in pore channel blockage, reduction in the amount, and unfavorable connectivity. By contrast, dissolution is the dominated diagenesis for the marine shale in the late diagenesis stage. The dissolved pore in carbonate develops that even has begun to connect and form a pore network system (Figs. 5(i) and 6(i)), has a positive contribution to PV and SSA. On the other hand, carbonate cementation damages the pore structure, and the coupling of them shows a weak positive correlation (Figs. 12(c) and 12(f)).

3.4 Control of diagenetic evolution on pore structure

The discrepancy of organic geochemical parameter and mineral composition characteristics among the three types of shale reservoirs leads to pore structure diversity. This is because that the old to new sedimentary period of the K_1s, C_2–P_1t–P_1x, and S_1l, the sedimentary diagenesis and diagenesis stage are diverse in different burial depth, which gives rise to different pore type and structure in shale (Figs. 5 and 6). Accordingly, in terms of reservoir diagenetic evolution, the effects of the thermal evolution of organic matter, clay mineral transformation, and diagenesis on pore structure are discussed. The R_o of the K_1s ranges from 0.77% to 1.01%, which is in the low mature- mature stage and located in the "oil window." The organic matter evolution is dominated by asphaltization and aromatization, forming oil and moisture principally. K_1s is in period A of the middle diagenetic stage. Compaction and cementation are the main affected factor during pore evolution. The primary pores are abundantly developed, composed of intergranular pore, and interlayer pore in clay, intergranular pore and stacked pore in brittle minerals. And a few secondary pores are found, consist of the dissolved pore, moldic pore, and the directional pore formed by pressure solution of brittle minerals. Since the favorable preservation of primary pores, PV and SSA have a positive linear correlation versus quartz, feldspar, and clay content, while a negative correlation versus calcite and dolomite content existed, caused by the cementation of carbonate. Additionally, the evolution of organic matter is lower, and the development of internal pores is poor, resulting in a weak linear negative correlation of pore structure parameters versus TOC (Fig. 13).

In the transitional shale (C_2–P_1t–P_1x), the R_o is in the range of 1.83%–2.1% (Generally in the high maturity stage), which has passed the limit of oil generation. And the evolution of organic matter is dominated by aromatization, cyclization, and pyrolysis, mainly forming wet gas and condensate gas. Source rock reservoir is in period B of the middle diagenetic stage. The pore evolution is chiefly controlled by dissolution, composed of residual primary pores and a certain amount of secondary pores. The former is consisting of an intergranular pore and interlayer pore in clay minerals basically, while the latter includes hydrocarbon generating pore of organic matter and a few microfissure in the edge of brittle mineral and organic matter (Figs. 5 and 6). However, the carbonate is negligible in transitional shale, the effect of cementation on the pores is weak, and the primary pores of clay minerals are well preserved (Fig. 13).

Moreover, a few dissolved pores are detected in feldspar and quartz. At this stage, the organic matter pore well developed due to the generation of gaseous hydrocarbons, PV and SSA have a positively correlated versus TOC, while the intergranular pore in brittle minerals was significantly affected by diagenetic evolution, PV and SSA have a negative linear correlation versus feldspar and quartz content. Although the pores in clay minerals were affected by compaction and cementation, interlayer pore and microfissure are still well developed. There was a positive linear correlation versus PV and SSA.

The R_o ranges from 2.0% to 2.84% in the S_1l shale, which is in the over maturity-high over maturity. The evolution of organic matter was dominated by pyrolysis (demethylation), principally forming dry gas, including a sea of oil cracking gas, reaching the peak of gas generation. In this process, the organic matter was acted by hydrocarbon generation expansion, and quite a few internal pores developed. Accordingly, the reservoir evolved to the late diagenetic stage. The pore types were dominated by secondary pore, consisting of organic matter pore, dissolved pore in carbonate, and microfissure in the edge of organic matter and brittle mineral (Figs. 5 and 6). Also, there is a spot of residual primary pores, mainly intergranular pores and intragranular pores of the clay and brittle minerals. Compared with continental and transitional shale, the development of the primary pore was getting worse gradually (Fig. 13).

In summary, the diagenetic evolution of the S_1l is relatively low in period A of the middle diagenesis stage. And the pore development is controlled by the primary pore, such as interlayer pore and intergranular pore of clay and intergranular pore of brittle mineral, while carbonate is not favorable to pore development affected by cementation. Transitional shale is in period B of the middle diagenesis stage. The pore development was controlled by residual primary pore in clay, organic matter pore, and marginal microfissure (secondary pore). And marine shale is in the late diagenesis stage, organic matter pore and marginal microfissure are widely developed, and carbonate dissolved pore is also well developed influenced by dissolution, while the residual clay mineral pores exhibit poor performance due to high diagenesis evolution. Notably, the S% in mixed

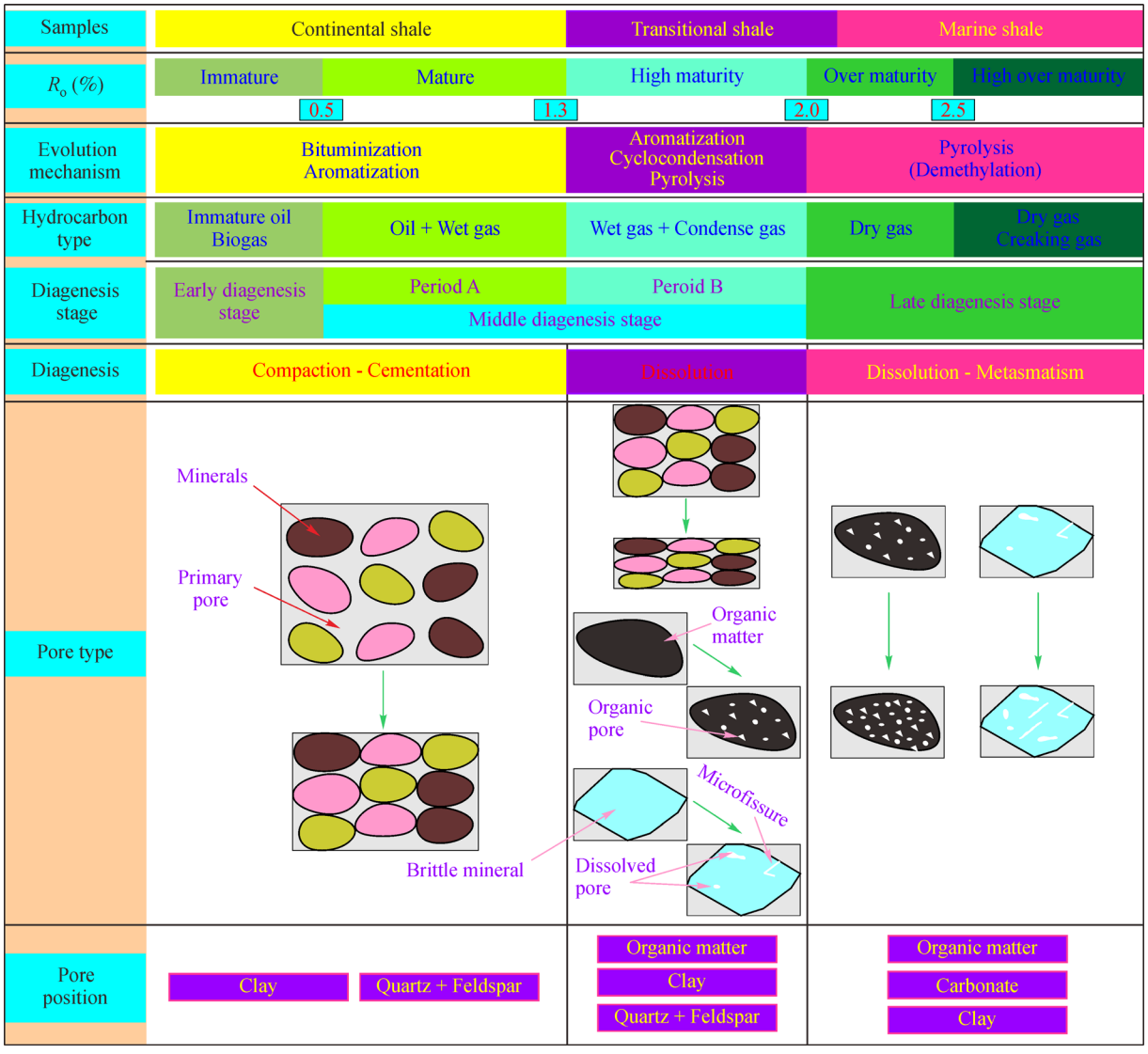

Fig. 13 Pore development characteristics and evolution model of continental, transitional, and marine shale samples.

I/S of transitional shale is lower than that of marine shale, contrary to the diagenetic evolution trend. The reason behind this phenomenon is the inhibition of kerogen evolution on clay mineral transformation. Although the pore performance of clay is poor in marine shale affected by compaction, the completion degree of smectite-illite transformation is lower than that of transitional shale. Consequently, the controlling mechanism of diagenetic evolution and diagenetic stage on the pore structure of shale is mainly reflected in two aspects, which are: (i) compaction and cementation destroy the primary pore, and (ii) dissolution and hydrocarbon generation of organic matter promote the formation of the secondary pore.

3.5 Implication on exploration and development of the three types of shale reservoirs

In this investigation, the thermal maturity of the K_1s is in the "oil window." Hence shale oil resources also should be focused on the exploration process. The thickness of the K_1s is large, the continuity of the reservoir is excellent, and it has certain development potential. In general, the TOC of the K_1s in the Jiaolai basin is relatively low, the hydrocarbon generation capacity and potential are medium. Consequently, in the exploration process, it is promised to detect the depositional center and subsidence center of the K_1s in each depression of the Basin, and explore the areas with high TOC and R_o, to realize the co-mining for oil and gas efficiently and economically. Transitional shale is in high maturity with a significant resource potential. And it coexists with coal-bearing sandstone and coal seam. Those form multiple sets of superimposed gas bearing systems of source- reservoir-caprock combination vertically. However, the single-layer thickness of transitional shale is thin, and the average clay content over 50%, which is not favorable to the process of

hydraulic fracturing.

Consequently, the fracturing effect is the critical factor restricting the production capacity. Suppose the shale gas mining technology can make revolutionary progress (e.g., the injection of supercritical CO_2 into shale reservoirs to enhance CH_4 recovery and realize CO_2 capture and storage). In that case, the limitations and disadvantages of the hydraulic fracturing process can be avoided. Then the transitional shale gas resources will be the next hot spots of the energy field. The commercial development of marine shale gas has been successfully realized in the Fuling, Changning, Zhaotong, and Taiyang blocks in southern China, which has been verified huge exploration and development potential, and the Guizhou, Guangxi, and other provinces are also in the exploration practice.

Nevertheless, the Longmaxi reservoir has suffered strong structural transformation in the Yanshanian and Himalayan (He et al., 2019; Peng et al., 2020), resulted in the preservation conditions are significantly distinct. Except for the source rock-reservoir performance, the caprock and trap conditions also captured wide attention. Comprehensively account for shale gas production and economic benefits, the principle of "high TOC, high-pressure coefficient, moderate buried depth, simple structure, and complete regional cap rock" should be followed.

4 Conclusions

1) TOC of continental shale samples is lower than that of transitional and marine shale samples. Marine shale recorded the highest quartz content, transitional shale recorded the highest clay content, and dolomite content was most remarkable in continental shale. The clay minerals in continental shale and marine shale are mainly illite and mixed I/S, while transitional shale contained a volume of kaolinite and chlorite.

2) PV and SSA of transitional and marine shale are slightly better than that of continental shale; transitional and marine shale have better development stability while continental shale has a greater range variety. PV in transitional and marine shale is mainly composed of micropore and mesopore (the proportion of macropore is lower); while micropore, mesopore, and macropore all have a significant contribution to continental shale. SSA of the three types of shale is mainly composed of micropore and mesopore; the proportion of macropore is negligible.

3) In the process of diagenetic evolution and diagenetic stage, compaction and cementation destroy the primary pores, including interlayer pore, intergranular pore of clay minerals, intergranular pore, and microfissure of brittle minerals. Dissolution and hydrocarbon generation of organic matter promotes the formation of the secondary pore, mainly including organic matter pore and dissolved pore in brittle minerals.

Acknowledgements This work is supported by the Major Project Cultivation of CUMT (No. 2020ZDPYMS09), the Foundation Research Project of National Science and Technology Major Project (No. 2017ZX05035004-002), and the Fundamental Research Funds for National Universities, China University of Geosciences (Wuhan).

References

Barth J M (2013). The economic impact of shale gas development on state and local economies: benefits, costs, and uncertainties. New Solut, 23(1): 85–101

Boyer C, Kieschnick J, Suarez-Rivera R, Lewis R E, Waters G (2006). Producing gas from its source. Oilfield Rev, 18(3): 36–49

Burnaman M D, Xia W W, Shelton J (2009). Shale gas play screening and evaluation criteria. China Petrol Explor, 14(3): 51–64

Chen G, Zhang H, Zhou L, Li X, Li X, LI S (2005). Relation between tectonics and the coupling coexistence of multiple energy resources in Ordos Basin. J Northwest U (Natural Science Edition), 35(6):783–786

Chen L, Jiang Z, Liu K, Tan J, Gao F, Wang P (2017). Pore structure characterization for organic-rich Lower Silurian shale in the Upper Yangtze Platform, south China: a possible mechanism for pore development. J Nat Gas Sci Eng, 46: 1–15

Chen Y, Ma D, Xia Y, Guo C, Shao K (2020). Characteristics of the mud shale reservoirs in coal-bearing strata and resources evaluation in the eastern margin of the Ordos Basin, China. Energ Explor Exploit, 38(2), 372–405

Colten-Bradley V A (1987). Role of pressure in smectite dehydration-effects on geopressure and smectite-to-illite transformation. Am Assoc Pet Geol Bull, 71(11): 1414–1427

Curtis M E, Cardott B J, Sondergeld C H, Rai C S (2012). Development of organic porosity in the Woodford Shale with increasing thermal maturity. Int J Coal Geol, 103: 26–31

Elliott W C, Edenfield A M, Wampler J M, Matisoff G, Long P (1999). The kinetics of the smectite to illite transformation in Cretaceous bentonites, Cerro Negro, New Mexico. Clays Clay Miner, 47(3): 286–296

Everett D H, Koopal L K. (2001). International union of pure and applied chemistry. Polymer, 31(8): 1598–1598

Fan A, Yang R, Lenhardt N, Wang M, Han Z, Li J, Li Y, Zhao Z (2019). Cementation and porosity evolution of tight sandstone reservoirs in the Permian Sulige gas field, Ordos Basin (central China). Mar Pet Geol, 103: 276–293

Gao F, Song Y, Li Z, Xiong F, Chen L, Zhang Y, Liang Z, Zhang X, Chen Z, Joachim M (2018). Lithofacies and reservoir characteristics of the Lower Cretaceous continental Shahezi Shale in the Changling Fault Depression of Songliao Basin, NE China. Mar Pet Geol, 98: 401–421

Ge T, Pan J, Wang K, Liu W, Mou P, Wang X (2020). Heterogeneity of pore structure of late Paleozoic transitional facies coal-bearing shale in the southern north China and its main controlling factors. Mar Pet Geol, 122: 104710

Guo C, Dong S, Zhong L (2019). Detrital zircon U-Pb geochronology of Upper Cambrian-Lower Silurian sandstone in the Wushi area, northwestern margin of Tarim Basin: implications for provenance

system and tectonic evolution. Acta Geol Sin, 93(11): 2759–2769

He D, Lu R, Huang H, Wang X, Jiang H, Zhang W (2019). Tectonic and geological setting of the earthquake hazards in the Changning shale gas development zone, Sichuan Basin, SW China. Pet Explor Dev, 46(5): 1051–1064

He Z, Nie H, Zhao J, Liu W, Bao F, Zhang W (2017). Types and origin of Nanoscale pores and fractures in Wufeng and Longmaxi shale in Sichuan Basin and its periphery. J Nanosci Nanotechnol, 17(9): 6626–6633

Ji L, Zhang T, Milliken K L, Qu J, Zhang X (2012). Experimental investigation of main controls to methane adsorption in clay-rich rocks. Appl Geochem, 27(12): 2533–2545

Jiang Z, Guo L, Liang C, Wang Y, Liu M (2013). Lithofacies and sedimentary characteristics of the Silurian Longmaxi Shale in the southeastern Sichuan Basin, China. J Palaeogeogr, 2(3): 238–251

Katsube T J, Williamson M A (1994). Effects of diagenesis on shale nano-pore structure and implications for sealing capacity. Clay Miner, 29(4): 451–461

Li Y, Nie H, Long P (2009). Development characteristics of organic-rich shale and strategic selection of shale gas exploration area in China. Nat Gas Industr, 29(12): 115–118 (in Chinese)

Li Y, Wang Z, Pan Z, Niu X, Yu Y, Meng S (2019). Pore structure and its fractal dimensions of transitional shale: a cross section from east margin of the Ordos Basin, China. Fuel, 241: 417–431

Li Y, Yang J, Pan Z, Tong W (2020). Nanoscale pore structure and mechanical property analysis of coal: an insight combining AFM and SEM images. Fuel, 260: 116352

Liang M, Wang Z, Li G, Gao L, Li C, Li H (2017). Evolution of pore structure in gas shale related to structural deformation. Fuel, 197: 310–319

Liu G, Zhai G, Zou C, Cheng L, Guo X, Xia X, Zhou Z (2019). A comparative discussion of the evidence for biogenic silica in Wufeng-Longmaxi siliceous shale reservoir in the Sichuan Basin, China. Mar Petrol Geol, 109: 70–87

Liu Z, Wang H, Man X (2015). Application of geological theory in shale gas exploration and development. Adv Mat Res, 1092–1093: 1346–1350

Long S, Peng Y, Liu H, Zhao C, Zhao J, Yu L, Sun C, Tang X (2017). Micro-Characteristics of the shale in the first member of Silurian Longmaxi Formation in southeastern Sichuan Basin, China. J Nanosci Nanotechnol, 17(9): 6662–6669

Loucks R G, Reed R M, Ruppel S C, Jarvie D M (2009). Morphology, genesis, and distribution of nanometer-scale pores in Siliceous mudstones of the Mississippian Barnett Shale. J Sediment Res, 79(12): 848–861

Pan J, Peng C, Wan X, Zheng D, Lv R, Wang K (2017). Pore structure characteristics of coal-bearing organic shale in Yuzhou Coalfield, China using low pressure N_2 adsorption and FESEM methods. J Petrol Sci Eng, 153: 234–243

Peng Y, Long S, He X, Tang J, Nie H, Gao Y, Xue G, Fan Y, Liu Y (2020). Characteristics of normal-pressure shale gas reservoirs and evaluation of its favorable areas in Penshui. Petrol Reserv Evaluat Developt, 10(05): 12–19

Qiu L (2018).Research on shale reservoir characteristics of Shuinan Formation in northern Jiaolai Basin. Dissertation for Doctoral Degree. Xuzhou: China University of Mining and Technology (in Chinese)

Song W, Yao J, Li Y, Sun H, Zhang L, Yang Y, Zhao J, Sui H (2016). Apparent gas permeability in an organic-rich shale reservoir. Fuel, 181: 973–984

Tian T, Wang H, Zheng R, Hou C, Wang C (2014). Low permeability reservoir characteristics of Chang 8 oil reservoir set in Zhenyuan area, Ordos Basin. Lithol Reserv, 26(1): 29–35 (in Chinese)

Wang M, Xie W, Huang K, Dai X (2019). Fine characterization of lithofacies and pore network structure of continental shale: case study of the Shuinan Formation in the north Jiaolai Basin, China. J Petrol Sci Eng, 175: 948–960

Xie W, Wang M, Wang X, Wang Y, Hu C (2021). Nano-pore structure and fractal characteristics of shale gas reservoirs: a case study of Longmaxi Formation in southeastern Chongqing, China. J Nanosci Nanotechn, 21: 343–353

Xiong F, Jiang Z, Chen J, Wang X, Huang Z, Liu G, Chen F, Li Y, Chen L, Zhang L (2016). The role of the residual bitumen in the gas storage capacity of mature lacustrine shale: a case study of the Triassic Yanchang shale, Ordos Basin, China. Mar Pet Geol, 69: 205–215

Xiong F, Jiang Z, Tang X, Li Z, Bi H, Li W, Yang P (2015). Characteristics and origin of the heterogeneity of the Lower Silurian Longmaxi marine shale in southeastern Chongqing, SW China. J Nat Gas Sci & Eng, 27(P3): 1389–1399

Yang W, Song Y, Jiang Z, Luo Q, Wang Q, Yuan Y, Zhang C, Chen L (2018). Whole-aperture characteristics and controlling factors of pore structure in the Chang 7 continental shale of the Upper Triassic Yanchang Formation in the southeastern Ordos Basin, China. Interpretation (Tulsa), 6(1): T175–T190

Zhang J, Li X, Xie Z, Li J, Zhang X, Sun K, Wang F (2018). Characterization of microscopic pore types and structures in marine shale: examples from the Upper Permian Dalong Formation, Northern Sichuan Basin, South China. J Nat Gas Sci Eng, 59: 326–342

Zhao C, Zhu X (2001). Sedimentary Petrology. 3rd ed. Beijing: Petroleum industry press

Zhao J, Jin Z, Jin Z, Geng Y, Wen X, Yan C (2016). Applying sedimentary geochemical proxies for paleoenvironment interpretation of organic-rich shale deposition in the Sichuan Basin, China. Int J Coal Geol, 163: 52–71

Zhao J, Jin Z, Jin Z, Geng Y, Wen X, Yan C (2017). Nano-scale pore characteristics of organic-rich Wufeng and Longmaxi Shales in the Sichuan Basin, China. J Nanosci Nanotechnol, 17(9): 6721–6731

Zhu X (2008). Sedimentary Petrology. Beijing: Petroleum Industry Press